Reversible conductance and surface polarity switching with synthetic molecular switches

Kumar, Sumit

DOI:
10.33612/diss.95753670

6

PHOTOSWITCHABLE CUCURBIT[8]URIL MONOLAYER ON GOLD SURFACE

*This chapter introduces the surface immobilization of a supramolecular cucubit[8]uril (**CB[8]**) complex with a light-responsive thread, bearing paraquat and azobenzene moieties, connected to surface anchoring group via tetraethylene glycol linker. The **CB[8]** complexes were grafted on Au(111) surface in a simple two-step process, that is, immobilization of the thread followed by complexation of the thread by the cavitand. Upon exposure of the surface-confined complex of UV light, the paraquat moiety is expelled from the cavitand but when irradieated with white light ($\geq 455nm$) it threads back into the macrocyle. The conformational change of molecular complex were analyzed by XPS and contact angle measurements and fatigue behaviour when moving in and out of the cavitand is analysed.*

Sumit Kumar, Wojciech Danowski, Laura Nunes dos Santos Comprido, Tasheen Zehra, Sander J. Wezenberg, Ben L. Feringa, and Petra Rudolf, "Maximized change in contact angle for photo-switchable cucurbit[8]uril-mediated supramolecular monolayers on gold", in preparation.

6.1. INTRODUCTION

Responsive functional surfaces, whose properties and function can be altered by an external stimulus, continue to attract significant attention for their application as sensors[1–4], biochips[5],lubricants[6–8], coatings[9–11], or electronic devices [12–15]. Photo-responsive molecular switches are among the most promising candidates for the fabrication of responsive functional surfaces as light, in comparison to other stimuli, offers the highest level of spatiotemporal control over the surface properties. The light-induced structural change of these molecules on surfaces can be exploited for switching wettability[16–22] or for opto-mechanical applications[14, 23]. Fabrication of photo-responsive self-assembled monolayers (SAMs) requires a good understanding of chemical and optical properties of the substrate. For the efficient switching of the photoactive SAM, a sufficient free volume around each switch is required, which can be achieved either by using a mixed monolayer strategy or a bulky anchoring group[12, 20, 24]. In addition, the lateral separation of the chromophores in the SAM prevents intermolecular exciton coupling between the adjacent photoswitches[25, 26]. The light-induced water contact angle (WCA) changes of currently known photoactive SAMs are modest, amounting to 2 – 14° for azobenzene monolayers [16, 21, 27], to 6 – 10° for spyropyrans[18, 21, 28], and to 5 – 7° for diarylethylenes[20]. Different approaches have been followed to amplify these changes, for example by increasing the surface roughness[17, 28–30] through grafting of polymer brushes to the surface[31–34], or fabrication of patterned surfaces[22]. Nevertheless, the control of the WCA on flat, non-patterned surfaces by light remains a fundamental challenge.

Recently a lot of attention has been devoted to the assembly of SAMs of photoresponsive host-guest complexes[35]. In these systems the isomerization of the photoswitch usually promotes the dissociation/association of the supramolecular complex and therefore, conformational change associated with the isomerization of the photoswitch can be further amplified, which in turn, should result in larger variation in WCA between the pristine and the irradiated surface[30, 36]. For this purpose, responsive surfaces functionalized with macrocyclic hosts including cyclodextrins[30, 36] and calixarenes[37] have been fabricated and were proven to exhibit large WCA changes modulated by light on rough or patterned surfaces.

As one of the largest macrocyclic hosts, cucubit[8]uril (**CB[8]**) can simultaneously accommodate up to two guest molecules within its hydrophobic cavity, in particular an electron poor paraquat ($\mathbf{MV}^{+2}$) and electron rich E-azobenzenes, forming a heteroternary photoswitchable complexs[38, 39]. A practical translation of this rich **CB[8]** host-guest chemistry to the surface confined systems, yielded functional, photoresponsive interfaces for the immobilization of micelles[40], coloids[41], polymer brushes[31], memory deivces[42] or light-modulation of adhesive properties[43, 44].Scherman et. al. showed that irradiation of the binary complex of azobenzenes, bearing an adjacent cations, and $\mathbf{MV}^{+2}$ **CB[8]** leads to expulsion of $\mathbf{MV}^{+2}$ from the **CB[8]** cavity due to much higher binding affinity of cationic Z−azobenzenes to **CB[8]** than that of $\mathbf{MV}^{+2}$ to **CB[8]**[45].

Inspired by this pioneering work, we considered this type of switchable inclusion complexes suitable candidates for fabrication of photoresponseive SAMs. In this chapter, we present, a simple design of a novel **CB[8]** guest comprising a cationic

azobenzene photoswitch and a paraquat moiety connected with tetraethyleneglycol to thiol anchoring group for suface modification. We envisioned that the hydrophilic tetraethylenglycol chain would orient the thread vertically to the relatively hydrophobic gold surface, while the bulky **CB[8]** would provide the free volume essential for effective switching in the surface confined system (Figure 6.1).

6.2. RESULTS AND DISCUSSION

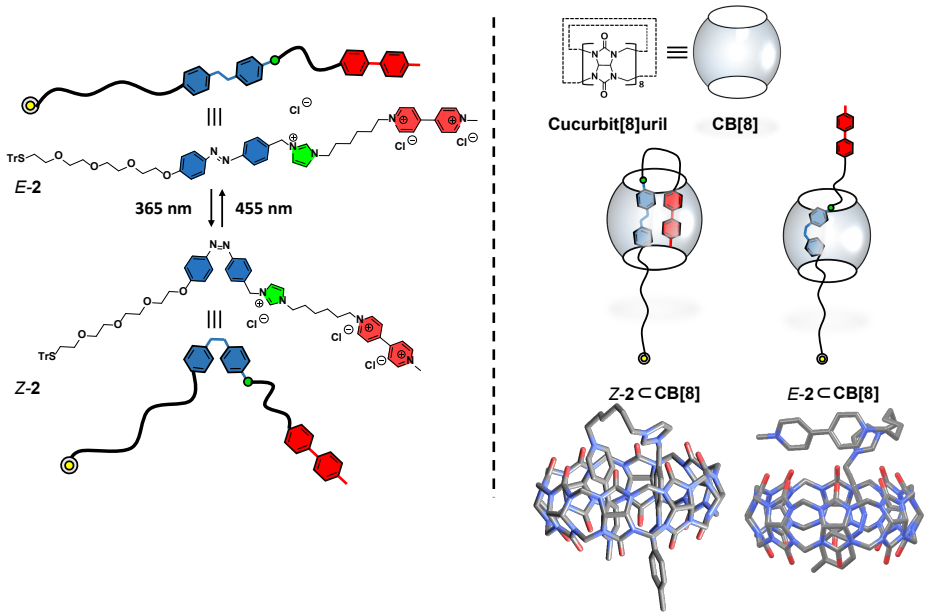

Figure 6.1 Schematic illustration of the design, structure and photoswitching of the trityl-protected azobenzene thread (E−2) (left panel) and photoswitching of the supramolecular photoresposive host-guest complex with *E*-2⊂**CB[8]** (right panel). The DFT optimized structures (M06-2X def2-TZVP (see appendix 7.4 for details) with SDM solvation model for wateer) of model photoswitchable supramolecular complexes (left lower panel).

6.2.1. PHOTOCHEMICAL ISOMERIZATION STUDIES IN SOLUTION

The photochemical E→Z isomerization of the E−2 ⊂**CB[8]** (Figure 6.2 (a),(c)) complex as well as of the trityl-protected thread E−2 (Figure6.2) alone were studied in solution by ^{1}HNMR by UV/Vis absorption spectroscopies. As expected, in the absence of **CB[8]**, the bare thread shows the typical isomerization behaviour of azobenzene photoswitches (Figure 6.2 (b)). In the UV/Vis absorption spectra, irradiation of the aqueous solution of E−2 at 365 nm led to a gradual decrease in the absorbance at 355 nm with a concomitant increase in the absorbance at 455 nm, in line with the E→Z isomerization of the azobenzene moiety (Figure 6.2 (b), red spectrum). The complementary Z→E isomerization could be achieved upon irradiation of Z−2 at

455 nm, which led to a gradual recovery of the original UV/Vis absorption (Figure 6.2 (b), blue spectrum).Reversible E-Z photoswitching of the bear thread could be performed for at least five cycles by alternating UV-Vis irradiations without any appreciable amount of fatigue (Figure 6.2 (b), inset). The composition of the photostationary state (PSS) mixtures formed upon sufficient irradiation at both wavelengths was determined from the ^{1}HNMR spectra. It was found that the E→Z photoisomerization of the bare thread proceeds almost quantitatively (PSS_{365} 95:5 of Z−2 :E−2), while the irradiation at 455 nm gives rise to a slightly lower ratio of configurational isomers (PSS_{455} 72:28 of Z−2 :E−2).

In the aqueous solution, the inclusion complex E−2 ⊂**CB[8]** was found to form almost immediately upon mixing of the E−2 thread with **CB[8]**. In fact, ^{1}HNMR spectroscopy revealed a significant upfield shift of the resonances ascribed to the aromatic protons of the paraquat and azobenzene moieties of the thread, consistent with the encapsulation of both these moieties in the hydrophobic interior of the **CB[8]** cavitand (Figure 6.2 (a), red spectrum, red and blue dashed lines respectively). When irradiated at 365 nm, the E−2 ⊂**CB[8]** host-guest complex showed a similar signature of the photoswitching behavior in the UV/Vis absorption spectrum as the free E−2 thread, namely a gradual decrease in the absorbance at 355 nm accompanied by small increase

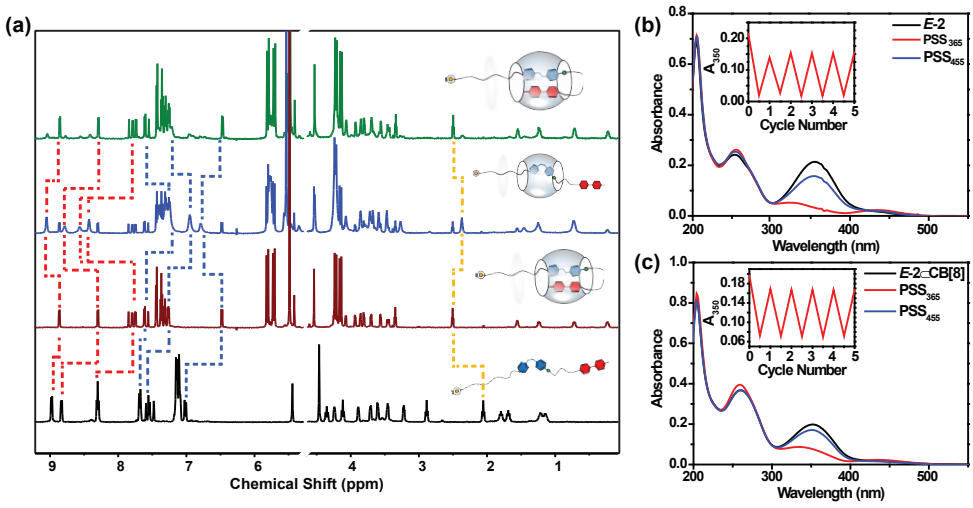

Figure 6.2 2. (a) Comparison of the ^{1}H NMR spectra (400 MHz, D2O, MeOH-d4) of bare thread E−2 (black spectrum), complex E−2 ⊂**CB[8]** (red spectrum), photostationary state mixture obtained by sufficient irradiation at 365 nm of E−2 ⊂**CB[8]** (PSS_{365}, blue spectrum), and photostationary state mixture obtained by sufficient irradiation at 365 nm of E−2 ⊂**CB[8]** (PSS_{455}, green spectrum). The dashed lines indicate changes in chemical shift of resonances ascribed to paraquat (red, dashed lines), azobenzene (blue, dashed lines) and methylene adjacent to thioether (yellow, dashed lines) protons. (b) Changes in UV/Vis absorption spectrum E−2 (black spectrum), after irradiation at 365 nm (PSS_{365}, red spectrum) and after consecutive irradiation with 455 nm (PSS_{455}, blue spectrum). (c) Changes in UV/Vis absorption spectrum E−2 ⊂**CB[8]** (black spectrum), after irradiation at 365 nm (PSS_{365}, red spectrum) and after consecutive irradiation with 455 nm (PSS_{455}, blue spectrum). The insets show the absorbance during multiple irradiation cycles.

in the absorbance at 455 nm, pointing to the E→Z isomerization of the azobenzene moiety encapsulated by **CB[8]** (Figure 6.2 (c)). In the ^{1}HNMR spectrum, irradiation at 365 nm of the aqueous solution of the E−2 ⊂**CB[8]**, (Figure 6.2 (a), blue spectrum) resulted in a significant downfield shift of the resonances of the protons ascribed to the paraquat moiety towards the positions observed for the bare thread (Figure 6.2 (a), black curve, red, dashed lines). This leads to the conclusion that formation of the Z-2⊂**CB[8]** complex entails expulsion of the paraquat moiety from the cavitand.

The complementary Z→E isomerization could be achieved through irradiation at 455 nm, which led to a gradual recovery of the E−2 ⊂**CB[8]** complex, as proven by the UV/Vis absorption and ^{1}HNMR spectra (Figure 6.2 (a), green spectrum). The reversible E→Z photoswitching of the supramolecular complex could be performed for at least five cycles by alternating UV and Vis irradiation without any appreciable sign of fatigue, as demonstrated by the intensity change of the 355 nm absorption during alternate illumination with 365 nm and 455 nm light shown as inset in the bottom right. From the composition of the photostationary state (PSS) mixtures (PSS_{365} ratio of 74 : 26 of Z-2⊂**CB[8]**: E−2 ⊂**CB[8]**) the E→Z isomerization of the encapsulated azobenzene thread was found to proceed with lower efficiency than that of the bare thread, while the complementary Z→E photoisomerization resulted more selective, giving rise to the much higher PSS ratio (PSS_{455} ratio of 10 : 90 of Z-2⊂**CB[8]**: E−2 ⊂**CB[8]**). Having established that in solution the photoisomerization of both bare and encapsulated threads proceeds in the same fashion and that the paraquat moiety moves in and out of the **CB[8]** host when stimulated by light, we undertook the fabrication of the photoresponsive supramolecular surface.

6.2.2. SURFACE FUNCTIONALIZATION

Surface functionalization with E−2 is rather challenging compared to the formation of self-assembled monolayers (SAMs) of simple molecules such as alkanethiols because these molecules are insoluble in a variety of solvents, and unstable in normal atmospheric conditions. We therefore prepared all samples under glove box conditions (1 ppm H_2O, 1 ppm O_2), and stored them in inert atmosphere before measurements. The switches were grafted on 100 nm Au deposited on mica (see experimental techniques for details). A methanolic solution of E−2 switches was prepared under glove box conditions by adding a few drops of tetrahydrofuran (THF). The solution was stirred for 5 min at room temperature before immersing a freshly prepared Au/mica substrate for 8 h; thereafter the samples were gently rinsed three times with methanol, dried in an Ar atmosphere and sealed in Ar atmosphere before characterization (**sample 1**) or immediately used to form complexes with **CB[8]**. For the latter, an aqueous dispersion of **CB[8]** was prepared in degassed DI water (resistivity >18 M Ω*cm) and sonicated for 40 min before immersing the freshly prepared **sample 1** for 5 min. Afterwards, the sample was rinsed with DI-water and dried under Ar atmosphere. These samples were either irradiated by white light (**sample 2**) or UV light (**sample 3**) in order to produce the conformations sketched in Figure 6.3 left panel - before being measured.

We used X-ray photoelectron spectroscopy (XPS) to check the integrity of the molecules on the two gold surfaces (**sample 1** and **sample 2**) and to follow the changes in conformation induced by irradiation in order to verify whether the model (**sample 3**)

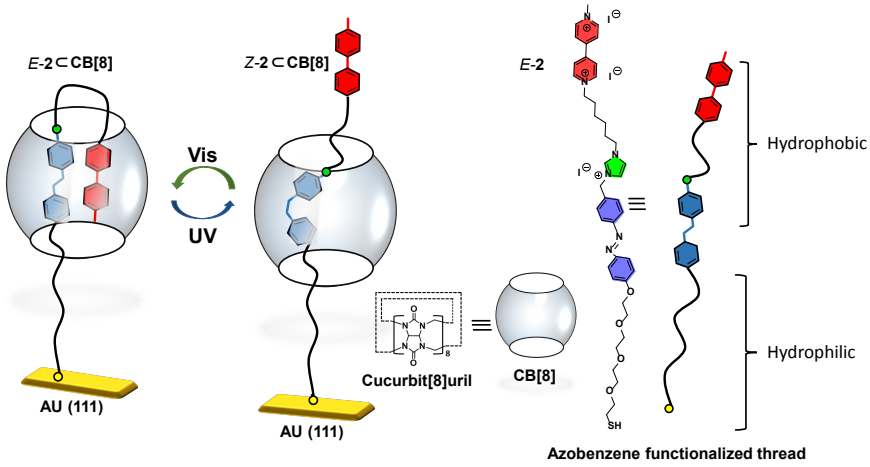

Figure 6.3 Right: Molecular structure of the photoswitchable azobenzene functionalized thread (E−2), and of cucurbit[8]uril (**CB[8]**). Left: Schematic diagram of the molecules (E−2 ⊂**CB[8]**) attached to the Au surface; under visible irradiation the photo-switchable molecules have cis form, and hence paraquat inserted inside the **CB[8]** cavitand while under UV radiation the molecule undergoes the transition to the trans form (Z-2⊂**CB[8]**) and the paraquat moity is expelled from the **CB[8]** cavity.

6

presented in Figure 6.3 is indeed correct. Nitrogen is present in both guest (E−2 thread) and host (**CB[8]**) molecules.Figure 6.4 (a),(b), and (c), presents the N1s core level spectra of **sample 1**, **2**, and **3**, respectively. The spectrum of **sample 1**, where the bare thread is grafted onto Au(111), comprises three distinguishable components (Figure 6.4 (c)); the first one at a binding energy of 399.8 eV [46], corresponds to nitrogen in the azobenzene moiety, N_{azo}, whereas the lower charge density on N^+ in the pyridinium moieties, N_{pqt}, gives rise to the component at 401.0 eV[12, 47]. The third component at 402.3 eV can be attributed to N^+ in the five membered ring in imidazolium, N_{imz}, where the charge density around the photoemitting nitrogen is lowest. These components contribute with 40±2% (N_{azo}), 22±3% (N_{pqt}) and 37±3% (N_{imz}) to the total N1s spectral intensity. The additional component at a binding energy of 400.2 eV[48], detected in the spectra of **sample 2** and **3** (presented in Figure 6.4 (b) and (a)), corresponds to N in an carbaminde group and confirms the presence of **CB[8]** moieties on these surfaces. In **sample 2**, N_{azo} peak sifted by 0.8 eV toward lower binding energy, because of hydrophobic interaction with the **CB[8]** core. Differences in intensity of the nitrogen components observed for **sample 2** and **3** (Figure 6.4 (a) and (b)) will be discussed below in the section on the switching mechanism.

Figure 6.5 presents the C1s, S2p and I3d XPS spectra of **sample 1**nd **2**. The C1s spectrum of **sample 1** (Figure 6.5 (b)) consists of three distinct components, one at a binding energy of 285.1 eV[49], originating from C-C bonds, a second one at 287.4 eV[50][51], corresponding to C-O-C bonds and a relatively broad one (with a full width at half maximum of 0.6 eV) at 286.4 eV[49], which stems from C=N-C, C-S and C-O bonds. After **sample 1** was exposed to **CB[8]** additional components at 287.9 eV[52] and

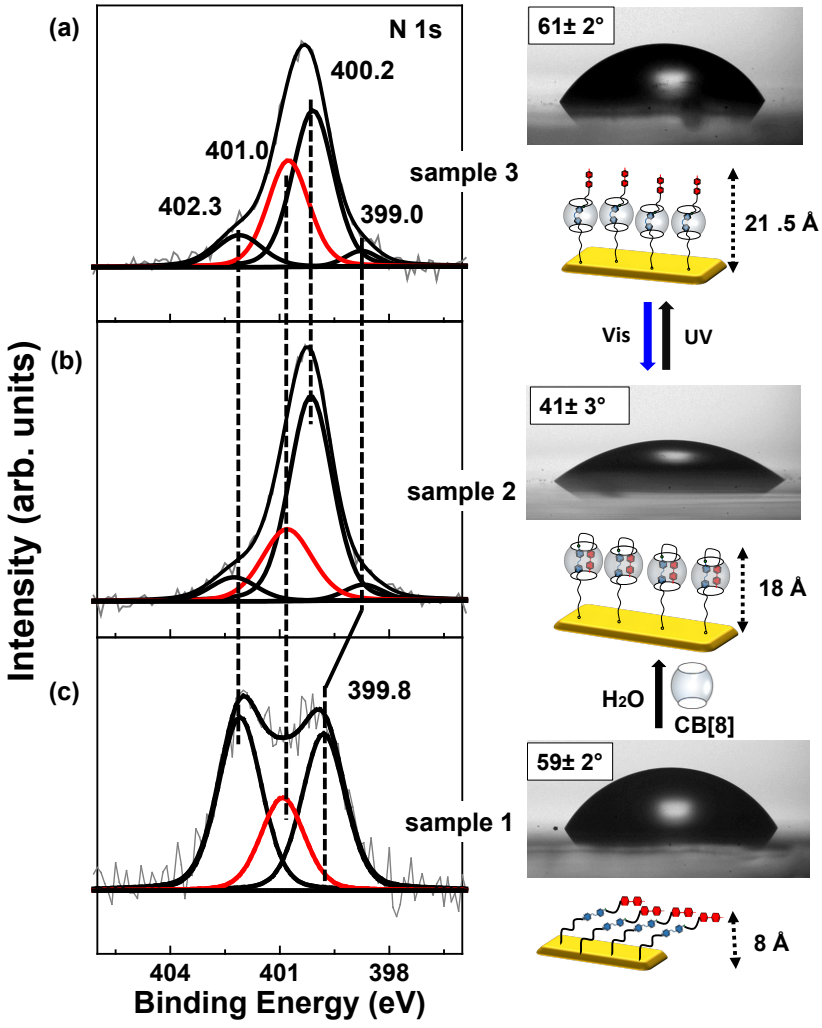

Figure 6.4 Left panels: XPS spectra of the N1s core level region collected from (c) a gold surface functionalized,with the azobenzene thread, sample 1; (b) the same surface after further modification with **CB[8]** and irradiation with visible ($\geqslant 455nm$) light, sample 2; and (a) the sample of spectrum (b) after irradiation with 365 nm light, sample 3. Right panels: Contact angles measured on the samples 1, 2 and 3, whose respective XPS are shown in the left panels and sketches of the presumed surface conformation of the grafted molecules in each case.

289.4 eV[48] appear in the C1s spectrum, testifying to the presence of N-(C=O)-N, and C-N-C species (Figure 6.5 (a)), and hence confirming that **CB[8]** adsorbed on the surface of **sample 2**.

The S2p core level spectra (Figure 6.5 (c) and (d)) consist of two doublets peaked at 161.8 eV[53] and 163.6 eV[12], which correspond to chemisorbed sulfur and disulphide

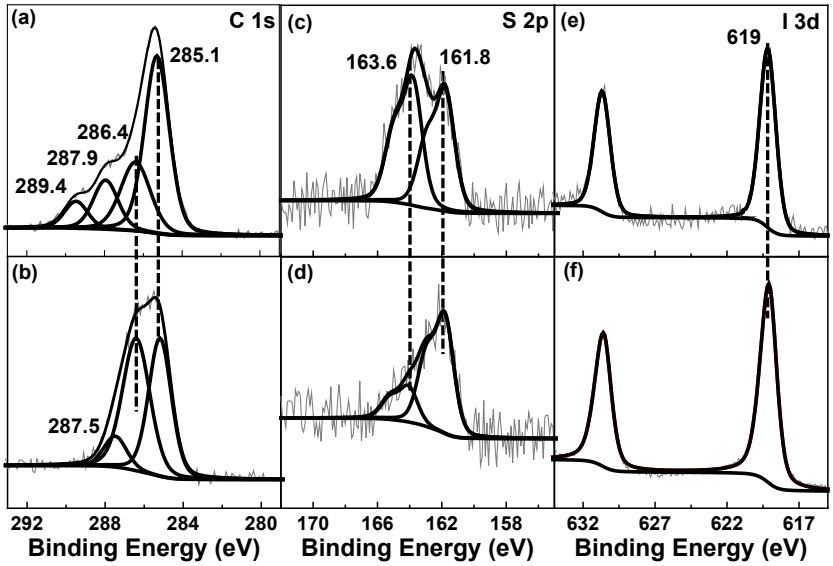

Figure 6.5 XPS spectra of the C1s, S2p and I3d core level regions collected from collected from (bottom panel) a gold surface functionalized,with the azobenzene thread, **sample 1**; (top panel) the same surface after further modification with **CB[8]** and irradiation with visible (⩾455 nm) light, **sample 2**.

6

bonds, respectively. The relative S2p photoemission intensity of sulfur in disulfide bonds changed from 20±2% to 48±3% after we functionalized **sample 1** with **CB[8]** in water (Figure 6.5 (c)). The I3d core level spectra (Figure 6.5 (e) and (f)) confirm the presence of the iodine anion on the azobenzene functionalized thread after grafting to the gold surface (**sample 1**) and after further functionalization with **CB[8]** and testify to the thread's integrity.

From the XPS spectra we can therefore conclude that our surface functionalization protocol was successful, resulting the adsorption of the E−2 switches on the Au(111) surface and the successive attachment of **CB[8]**. In the following we examine our evidence for **CB[8]** being actually threaded onto the E−2 switch and for the light-induced switching leading to the conformational changes sketched in Figure 6.3.

6.2.3. MECHANISM OF SURFACE SWITCHING

The theoretical length of the bare thread is 42 Å , whereas the length deduced from the attenuation the Au4f signal in the XPS spectrum of the E−2 molecules on the surface was 8.0±0.2 Å . This thickness of the molecular film on top of the gold surface in **sample 1** clearly indicates that the molecules are not tightly packed. The presence of the PEG chains may lead to a glassy phase structured like polymer brushes[54]. The molecular structure of **CB[8]** translates into a height of 9 Å [38] for the guest molecules, whereas the thickness of the surface-anchored the host-guest complex as deduced from the attenuation the Au4f signal in the XPS spectrum was 18.0 ±0.6Å . In other words, the modification of **sample 1** with the guest molecule and irradiation with visible

(⩾455 nm) light resulted in **sample 2** with an around ≈11 Å thicker adsorbate layer than **sample 1**, which is more than the height of the **CB[8]** molecules. To understand this conformational change we resorted to contact angle measurements, keeping in mind, as already mentioned earlier, that the **CB[8]** molecules have a hydrophobic core and a hydrophilic top outer rim. The images of water droplets on the various surfaces are shown in the right panel of Figure 6.4, where also the measured contact angle and the proposed structure are reported; the measured contact angles are also summarized in Table6.1 below. The water contact angle of **sample 1** was 59±2° at room temperature (see Figure 6.3, right panel), which agrees with a conformation like the one sketched in Figure 6.4, where the hydrophobic paraquat moieties are partially folded back. When **sample 1** is exposed to the host molecules, these hydrophobic moieties can bind to the hydrophobic cavity of **CB[8]**, as observed by NMR for the molecules in solution (Figure 6.2). The water contact angle of **sample 2** was measured to be 41±3° (Figure 6.4, right panel, center), which indicates that **sample 2** has a more hydrophilic surface than **sample 1** and supports the conformation drawn in Figure 6.3 (left panel, E−2 ⊂**CB[8]**) and Figure 6.4, where the **CB[8]** molecules arrange such that the hydrophilic top outer rim is facing away from the gold substrate, the azobenzene is in the cis form and the paraquat moieties inserted inside the cavitand. As sketched in Figure 6.3 for **sample 2** these results also suggest that the molecular thread orients more perpendicular to the Au surface when **CB[8]** is present.

Table 6.1: The water contact angle measurement after Vis (⩾455 nm) and UV (365 nm) irradiation of different samples prepared on Au(111)

Sample name	**Droplet size 0.5 μl**	**Droplet size 1.0 μl**
Sample 1 after irradiation with visible light	61±3°	59±3°
Sample 1 after irradiation with UV light	58±2°	59±2°
Sample 2	45±2°	41±3°
Sample 3	60±3°	58±2°

After irradiation with 365 nm, UV light to produce the configuration sketched in Figure 6.3, the water contact angle changed to 61±2°, and the adsorbate layer thickness increased to 21.5±03 Å , in agreement with a conformation change as shown in Figure 6.4, (right panel top), where the azobenzene moiety underwent a cis to trans isomerism and the paraquat moiety was expelled from the cavity and exposed on the surface. The dynamic changes in the film thickness between **sample 2** and **sample 3** are only possible because the hydrophobic gold surface forces the lower hydrophilic PEG part of the thread to extend out from the surface, thereby also causing the hydrophobic part of the molecule to be available for threading by the cavitand as shown in Figure 6.3. In fact, the overall design of **CB[8]** molecules with their hydrophobic core and hydrophilic outer rim is such that various hydrophobic-hydrophilic interactions are possible giving rise to the conformational change, which results in the ≈20° water contact angle change in

response to irradiation with UV light. The summary of the contact angles of the different surfaces measured with different volume of the water droplet, reported Table6.1, shows that the ≈20° water contact angle change was reproducible for different samples.

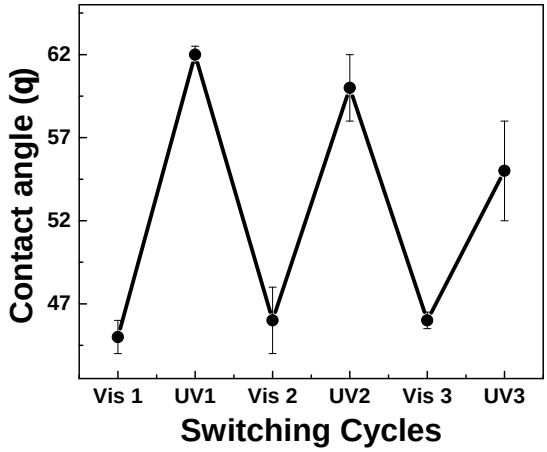

Figure 6.6 Switching cycles of E−2 ⊂**CB[8]** anchored on A(111) surface, monitored via contact angle of a 1 μL water droplet, measured after each alternate irradiation with 365 nm (UV) and ⩾455 nm (Vis) light (⩾455 nm)

We also studied the reversibility of the switching by measuring the water contact angle; the results during various switching cycles are shown in Figure 6.6. **Sample 2** with a contact angle of 45±2° was first irradiated with 365 nm UV light to generate **sample 3** with a contact angle of 62±3°. Irradiation with (⩾455 nm) visible light reverses the surface back to the initial conformation as seen from the contact angle of 46±3°, but if the alternate irradiations are continued, fatigue sets[55] in after the second cycle and the contact angle change becomes much less (see in Figure 6.6).

6.3. CONCLUSION

In summary, we synthesized a new supramolecular switch and demonstrated that it changes its conformation when stimulated by light both in solution when anchored to a surface. The switching behavior of the host–guest complex was carefully analyzed by ^{1}HNMR and UV/Vis absorption spectroscopy in solution as well as by XPS and contact angle measurements on the surface. In solution complex formation and multiple switching without any fatigue could be demonstrated. On the gold surface the E−2 switch adsorbs integer but forms a glassy disordered phase, rather than a densely packed self-assembled monolayer. However surface switching could be proven by the water contact angle change. The E−2 switch on the surface can be efficiently functionalized with **CB[8]**, and the complex shows a clear switching behavior under UV irradiation, which results in a water contact angle change of 20°. Most interestingly,

the switch is fully reversible under irradiation with visible light during fist cycle and the initial hydrophobicity of the surface is recovered. Moreover the observed changes in the thickness of the adsorbate layer upon illumination demonstrate that this surface mounted supramolecular system shows unprecedented dynamical behavior. In detail, the paraquat fragment moves out of the **CB[8]** macrocyle and threads back into it under alternate irradiation with UV and visible light, respectively.

BIBLIOGRAPHY

[1] J. Rickert, T. Weiss, and W. Göpel, "Self-assembled monolayers for chemical sensors: molecular recognition by immobilized supramolecular structure," *Sensors and Actuators B: Chemical*, vol. 31, no. 1, pp. 45 – 50, 1996. .

[2] S.-Y. Leo, W. Zhang, Y. Zhang, Y. Ni, H. Jiang, C. Jones, P. Jiang, V. Basile, and C. Taylor, "Chromogenic photonic crystal sensors enabled by multistimuli-responsive shape memory polymers," *Small*, vol. 14, no. 12, p. 1703515, 2018.

[3] R. Zhang, Q. Wang, and X. Zheng, "Flexible mechanochromic photonic crystals: routes to visual sensors and their mechanical properties," *Journal of Materials Chemistry C*, vol. 6, pp. 3182–3199, 2018.

[4] A. Abdollahi, A. Mouraki, M. H. Sharifian, and A. R. Mahdavian, "Photochromic properties of stimuli-responsive cellulosic papers modified by spiropyran-acrylic copolymer in reusable ph-sensors," *Carbohydrate Polymers*, vol. 200, pp. 583 – 594, 2018.

[5] T. Vo-Dinh, "Development of a DNA biochip: principle and applications," *Sensors and Actuators B: Chemical*, vol. 51, no. 1, pp. 52 – 59, 1998.

[6] J. Yang, H. Chen, S. Xiao, M. Shen, F. Chen, P. Fan, M. Zhong, and J. Zheng, "Salt-responsive zwitterionic polymer brushes with tunable friction and antifouling properties," *Langmuir*, vol. 31, no. 33, pp. 9125–9133, 2015.

[7] B. L. Wang, L. Heng, and L. Jiang, "Temperature-responsive anisotropic slippery surface for smart control of the droplet motion," *ACS Applied Materials & Interfaces*, vol. 10, no. 8, pp. 7442–7450, 2018.

[8] K. Han, L. Heng, Y. Zhang, Y. Liu, and L. Jiang, "Slippery surface based on photoelectric responsive nanoporous composites with optimal wettability region for droplets' multifunctional manipulation," *Advanced Science*, vol. 6, no. 1, p. 1801231, 2019.

[9] A. J. J. Kragt, D. J. Broer, and A. P. H. J. Schenning, "Easily processable and programmable responsive semi-interpenetrating liquid crystalline polymer network coatings with changing reflectivities and surface topographies," *Advanced Functional Materials*, vol. 28, no. 6, p. 1704756, 2018.

[10] Z. Dang, L. Liu, Y. Li, Y. Xiang, and G. Guo, "In situ and ex situ ph-responsive coatings with switchable wettability for controllable oil/water separation," *ACS Applied Materials & Interfaces*, vol. 8, no. 45, pp. 31281–31288, 2016.

[11] K. Chen, S. Zhou, S. Yang, and L. Wu, "Fabrication of all-water-based self-repairing superhydrophobic coatings based on uv-responsive microcapsules," *Advanced Functional Materials*, vol. 25, no. 7, pp. 1035–1041, 2015.

[12] S. Kumar, J. T. van Herpt, R. Y. N. Gengler, B. L. Feringa, P. Rudolf, and R. C. Chiechi, "Mixed monolayers of spiropyrans maximize tunneling conductance switching by photoisomerization at the molecule–electrode interface in egain junctions," *Journal of the American Chemical Society*, vol. 138, no. 38, pp. 12519–12526, 2016.

[13] A. S. Kumar, T. Ye, T. Takami, B.-C. Yu, A. K. Flatt, J. M. Tour, and P. S. Weiss, "Reversible photo-switching of single azobenzene molecules in controlled nanoscale environments," *Nano Letters*, vol. 8, no. 6, pp. 1644–1648, 2008.

[14] Y. Wen, W. Yi, L. Meng, M. Feng, G. Jiang, W. Yuan, Y. Zhang, H. Gao, L. Jiang, and Y. Song, "Photochemical-controlled switching based on azobenzene monolayer modified silicon (111) surface," *The Journal of Physical Chemistry B*, vol. 109, no. 30, pp. 14465–14468, 2005.

[15] V. Ferri, M. Elbing, G. Pace, M. D. Dickey, M. Zharnikov, P. Samorì, M. Mayor, and M. A. Rampi, "Light-powered electrical switch based on cargo-lifting azobenzene monolayers," *Angewandte Chemie International Edition*, vol. 47, no. 18, pp. 3407–3409, 2008.

[16] S. Wang, Y. Song, and L. Jiang, "Photoresponsive surfaces with controllable wettability," *Journal of Photochemistry and Photobiology C: Photochemistry Reviews*, vol. 8, no. 1, pp. 18 – 29, 2007.

[17] N. Delorme, J.-F. Bardeau, A. Bulou, and F. Poncin-Epaillard, "Azobenzene containing monolayer with photoswitchable wettability," *Langmuir*, vol. 21, no. 26, pp. 12278–12282, 2005. PMID: 16343003.

[18] D. Dattilo, L. Armelao, G. Fois, G. Mistura, and M. Maggini, "Wetting properties of flat and porous silicon surfaces coated with a spiropyran," *Langmuir*, vol. 23, no. 26, pp. 12945–12950, 2007.

[19] B. Xin and J. Hao, "Reversibly switchable wettability," *Chemical Society Reviews*, vol. 39, pp. 769–782, 2010.

[20] K.-Y. Chen, O. Ivashenko, G. T. Carroll, J. Robertus, J. C. M. Kistemaker, G. London, W. R. Browne, P. Rudolf, and B. L. Feringa, "Control of surface wettability using tripodal light-activated molecular motors," *Journal of the American Chemical Society*, vol. 136, no. 8, pp. 3219–3224, 2014.

[21] R. Rosario, D. Gust, M. Hayes, F. Jahnke, J. Springer, and A. A. Garcia, "Photon modulated wettability changes on spiropyran-coated surfaces," *Langmuir*, vol. 18, no. 21, pp. 8062–8069, 2002.

[22] W. Jiang, G. Wang, Y. He, X. Wang, Y. An, Y. Song, and L. Jiang, "Photo-switched wettability on an electrostatic self-assembly azobenzene monolayer," *Chemical Communications*, pp. 3550–3552, 2005.

[23] R. Turanský, M. Konôpka, N. L. Doltsinis, I. Štich, and D. Marx, "Optical, mechanical, and opto-mechanical switching of anchored dithioazobenzene bridges," *ChemPhysChem*, vol. 11, no. 2, pp. 345–348, 2010.

[24] T. Moldt, D. Brete, D. Przyrembel, S. Das, J. R. Goldman, P. K. Kundu, C. Gahl, R. Klajn, and M. Weinelt, "Tailoring the properties of surface-immobilized azobenzenes by monolayer dilution and surface curvature," *Langmuir*, vol. 31, no. 3, pp. 1048–1057, 2015.

[25] C. Gahl, R. Schmidt, D. Brete, E. R. McNellis, W. Freyer, R. Carley, K. Reuter, and M. Weinelt, "Structure and excitonic coupling in self-assembled monolayers of azobenzene-functionalized alkanethiols," *Journal of the American Chemical Society*, vol. 132, no. 6, pp. 1831–1838, 2010.

[26] M. Utecht, T. Klamroth, and P. Saalfrank, "Optical absorption and excitonic coupling in azobenzenes forming self-assembled monolayers: a study based on density functional theory," *Physical Chemistry Chemical Physics*, vol. 13, pp. 21608–21614, 2011.

[27] N. Delorme, J. F. Bardeau, A. Bulou, and F. Poncin-Epaillard, "Azobenzene-containing monolayer with photoswitchable wettability," *Langmuir*, vol. 21, no. 26, pp. 12278–12282, 2005.

[28] R. Rosario, D. Gust, A. A. Garcia, M. Hayes, J. L. Taraci, T. Clement, J. W. Dailey, and S. T. Picraux, "Lotus effect amplifies light-induced contact angle switching," *The Journal of Physical Chemistry B*, vol. 108, no. 34, pp. 12640–12642, 2004.

[29] R. Klajn, "Immobilized azobenzenes for the construction of photoresponsive materials," *Pure and Applied Chemistry*, vol. 82, no. 12, pp. 2247–2276, 2010.

[30] P. Wan, Y. Jiang, Y. Wang, Z. Wang, and X. Zhang, "Tuning surface wettability through photocontrolled reversible molecular shuttle," *Chemical Communications*, pp. 5710–5712, 2008.

[31] C. Hu, F. Tian, Y. Zheng, C. S. Y. Tan, K. R. West, and O. A. Scherman, "Cucurbit[8]uril directed stimuli-responsive supramolecular polymer brushes for dynamic surface engineering," *Chemical Science*, vol. 6, pp. 5303–5310, 2015.

[32] S. Samanta and J. Locklin, "Formation of photochromic spiropyran polymer brushes via surface-initiated, ring-opening metathesis polymerization: Reversible photocontrol of wetting behavior and solvent dependent morphology changes," *Langmuir*, vol. 24, no. 17, pp. 9558–9565, 2008.

[33] D. Wang, G. Ye, X. Wang, and X. Wang, "Graphene functionalized with azo polymer brushes: Surface-initiated polymerization and photoresponsive properties," *Advanced Materials*, vol. 23, no. 9, pp. 1122–1125, 2011.

[34] A. A. Brown, O. Azzaroni, and W. T. S. Huck, "Photoresponsive polymer brushes for hydrophilic patterning," *Langmuir*, vol. 25, no. 3, pp. 1744–1749, 2009.

[35] Y. Sun, J. Ma, D. Tian, and H. Li, "Macroscopic switches constructed through host–guest chemistry," *Chemical Communications*, vol. 52, pp. 4602–4612, 2016.

[36] Q. Shen, L. Liu, and W. Zhang, "Fabrication of a photocontrolled surface with switchable wettability based on host–guest inclusion complexation and protein resistance," *Langmuir*, vol. 30, no. 31, pp. 9361–9369, 2014.

[37] X. Zhang, H. Zhao, D. Tian, H. Deng, and H. Li, "A photoresponsive wettability switch based on a dimethylamino calix[4]arene," *Chemistry – A European Journal*, vol. 20, no. 30, pp. 9367–9371, 2014.

[38] S. J. Barrow, S. Kasera, M. J. Rowland, J. del Barrio, and O. A. Scherman, "Cucurbituril-based molecular recognition," *Chemical Reviews*, vol. 115, no. 22, pp. 12320–12406, 2015.

[39] J. del Barrio, S. T. J. Ryan, P. G. Jambrina, E. Rosta, and O. A. Scherman, "Light-regulated molecular trafficking in a synthetic water-soluble host," *Journal of the American Chemical Society*, vol. 138, no. 18, pp. 5745–5748, 2016.

[40] C. Hu, Y. Zheng, Z. Yu, C. Abell, and O. A. Scherman, "Surface-immobilised micelles via cucurbit[8]uril-rotaxanes for solvent-induced burst release," *Chemical Communications*, vol. 51, pp. 4858–4860, 2015.

[41] F. Tian, N. Cheng, N. Nouvel, J. Geng, and O. A. Scherman, "Site-selective immobilization of colloids on Au substrates via a noncovalent supramolecular handcuff," *Langmuir*, vol. 26, no. 8, pp. 5323–5328, 2010.

[42] F. Tian, D. Jiao, F. Biedermann, and O. A. Scherman, "Orthogonal switching of a single supramolecular complex," *Nature Communications*, vol. 3, p. 1207, 2012. Article.

[43] J. Liu, C. S. Y. Tan, and O. A. Scherman, "Dynamic interfacial adhesion through cucurbit[n]uril molecular recognition," *Angewandte Chemie International Edition*, vol. 57, no. 29, pp. 8854–8858, 2018.

[44] J. Liu and O. A. Scherman, "Cucurbit[n]uril supramolecular hydrogel networks as tough and healable adhesives," *Advanced Functional Materials*, vol. 28, no. 21, p. 1800848, 2018.

[45] J. del Barrio, P. N. Horton, D. Lairez, G. O. Lloyd, C. Toprakcioglu, and O. A. Scherman, "Photocontrol over cucurbit[8]uril complexes: Stoichiometry and supramolecular polymers," *Journal of the American Chemical Society*, vol. 135, no. 32, pp. 11760–11763, 2013.

[46] R. K. Layek and A. K. Nandi, "A review on synthesis and properties of polymer functionalized graphene," *Polymer*, vol. 54, no. 19, pp. 5087 – 5103, 2013.

[47] J. H. Ryu, D. O. Shin, and K.-D. Suh, "Preparation of a reflective-type electrochromic device based on monodisperse, micrometer-size-range polymeric microspheres and viologen pendants," *Journal of Polymer Science Part A: Polymer Chemistry*, vol. 43, no. 24, pp. 6562–6572, 2005.

[48] W. Zhu, W. Li, C. Wang, J. Cui, H. Yang, Y. Jiang, and G. Li, "Cb[8]-based rotaxane as a useful platform for sensitive detection and discrimination of explosives," *Chemical Science*, vol. 4, pp. 3583–3590, 2013.

[49] O. Ivashenko, J. van Herpt, B. Feringa, W. Browne, and P. Rudolf, "Rapid reduction of self-assembled monolayers of a disulfide terminated para-nitrophenyl alkyl ester on roughened au surfaces during XPS measurements," *Chemical Physics Letters*, vol. 559, pp. 76 – 81, 2013.

[50] B. Sivaranjini, R. Mangaiyarkarasi, V. Ganesh, and S. Umadevi, "Vertical alignment of liquid crystals over a functionalized flexible substrate," *Scientific Reports*, vol. 8, no. 1, p. 8891, 2018.

[51] S. Essa, J. M. Rabanel, and P. Hildgen, "Effect of polyethylene glycol (PEG) chain organization on the physicochemical properties of poly(d, l-lactide) (PLA) based nanoparticles," *European Journal of Pharmaceutics and Biopharmaceutics*, vol. 75, no. 2, pp. 96 – 106, 2010.

[52] N. Tawil, E. Sacher, E. Boulais, R. Mandeville, and M. Meunier, "X-ray photoelectron spectroscopic and transmission electron microscopic characterizations of bacteriophage–nanoparticle complexes for pathogen detection," *The Journal of Physical Chemistry C*, vol. 117, no. 40, pp. 20656–20665, 2013.

[53] O. Ivashenko, J. T. van Herpt, B. L. Feringa, P. Rudolf, and W. R. Browne, "Electrochemical write and read functionality through oxidative dimerization of spiropyran self-assembled monolayers on gold," *The Journal of Physical Chemistry C*, vol. 117, no. 36, pp. 18567–18577, 2013.

[54] M. A. C. Stuart, W. T. S. Huck, J. Genzer, M. Müller, C. Ober, M. Stamm, G. B. Sukhorukov, I. Szleifer, V. V. Tsukruk, M. Urban, F. Winnik, S. Zauscher, I. Luzinov, and S. Minko, "Emerging applications of stimuli-responsive polymer materials," *Nature Materials*, vol. 9, p. 101, 2010.

[55] G. Fang, Y. Shi, J. E. Maclennan, D. M. Walba, and N. A. Clark, "Photodegradation of azobenzene-based self-assembled monolayers characterized by in-plane birefringence," *Langmuir*, vol. 27, no. 17, pp. 10407–10411, 2011.